THE JOURNAL OF PHYSICAL CHEMISTRY B

Article

pubs.acs.org/JPCB

Molecular Interaction of Rifabutin on Model Lung Surfactant Monolayers

Marina Pinheiro,[†] Marlene Lúcio,[†,*] Salette Reis,[†] José L. F. C. Lima,[†] João M. Caio,[∥] Cristina Moiteiro,[∥] María T. Martín-Romero,[‡] Luis Camacho,[‡] and Juan J. Giner-Casares*[,‡,§]

[†]REQUIMTE, Departamento de Ciências Químicas, Faculdade de Farmácia, Universidade do Porto, Portugal

[‡]Department of Physical Chemistry and Applied Thermodynamics, University of Córdoba, Campus de Rabanales, Edificio Marie Curie, Córdoba, Spain E-14014

[§]Department of Interfaces, Max Planck Institute of Colloids and Interfaces, Science Park Golm, 14476 Potsdam, Germany

[∥]CQB, Departamento de Química e Bioquímica, Faculdade de Ciências, Universidade de Lisboa, Portugal

ABSTRACT: Tuberculosis is one of the most relevant problems for global health care. The design of new drugs against tuberculosis is aimed at maximizing impact against the disease, as well as minimizing the toxicological effect on the lung surfactant. In this work, the antituberculosis drug Rifabutin is studied in combination with phospholipid Langmuir monolayers as models of the lung surfactant monolayer. The zwitterionic 1,2-dipalmitoyl-*sn*-glycero-3-phosphocholine (DPPC) and the anionic 1,2-dipalmitoyl-*sn*-glycero-3-phospho-(1′-rac-glycerol) (DPPG) were used as model phospholipids. A combination of in situ experimental techniques of Brewster angle microscopy, polarization-modulated infrared reflection−absorption spectroscopy, and UV−vis reflection spectroscopy with computer simulations has been used. The interactions between Rifabutin and the DPPC and DPPG Langmuir monolayers were described as the formation of an inclusion complex. The phospholipid−Rifabutin inclusion complex prevents the penetration of the Rifabutin into the alkyl chain region of the phospholipids, leading to a disruption of the monolayer structure and a possible toxicological effect.

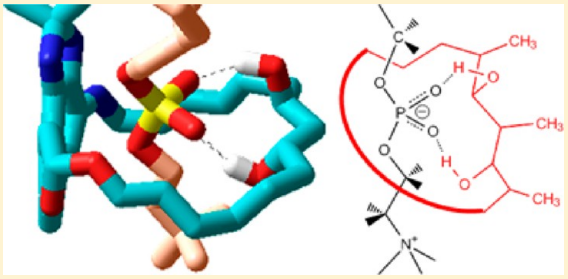

INTRODUCTION

Tuberculosis (TB) is a major problem for current global health care. TB is an infectious disease caused by the bacillus *Mycobacterium tuberculosis* (MTB). TB typically affects the lungs (pulmonary TB) but can affect other sites as well (extrapulmonary TB). TB affects mostly adults in the economically productive age groups; around two-thirds of cases are estimated to occur among people aged between the age of 15 and 59. In 2010, there were ca. 8.8 million incident cases of TB, ca. 1.1 million deaths from TB among HIV-negative people, and an additional 0.35 million deaths from HIV-associated TB.[1,2]

Intensive research is devoted to the development of new drugs against TB. Rifabutin (RBT) is an antituberculosis drug in current use, with a widespread use in the clinical practice.[3] RBT has been used as the starting structure for new derivatives as promising molecules against TB.[4] The rationale design of more efficient derivatives of RBT against TB would benefit from a deeper understanding of the molecular mechanism of action of RBT in the lung surfactant monolayer. Indeed, the lung surfactant monolayer presents several important functions by contributing to the small airway permeability, improving the mucocilliary depuration, and protecting against inhaled pathogens and injury, avoiding inflammation and oxidation.[5,6] Furthermore, due to its role in decreasing alveoli surface tension, the lung surfactant facilitates respiratory work and prevents alveoli collapse.[7,8] Hence, a low level of toxicity, i.e., low impact of the drug on the biophysical integrity of lung surfactant monolayer, is most desirable. Beyond evidence that indicates the importance of assuring the biophysical integrity of lung surfactant, the knowledge of interactions of drugs with this physiological barrier is scarce. Literature is particularly poor in information related to drugs accessibility and interaction with the lipid content of this barrier. Previous studies deal with the interactions of RBT with 3D models, such as multilamellar and unilamellar phospholipid vesicles.[9,10] However, the first steps in the interaction of RBT with the components of the lung surfactants occur at the monolayer/drug interface.

To this end, the study presented herein aims at the understanding of the interactions of RBT with a mimetic model of the lung surfactant, i.e., Langmuir monolayers formed by the most abundant lipid components in the inner interface of the lungs: 1,2-dipalmitoyl-*sn*-glycero-3-phosphocholine (DPPC) and 1,2-dipalmitoyl-*sn*-glycero-3-phospho-(1′-rac-glycerol) (DPPG) phospholipids.[11] At physiological pH, DPPC is in zwitterionic form, bearing no net charge, whereas DPPG is in

Received: April 18, 2012
Revised: August 17, 2012
Published: August 29, 2012

   dx.doi.org/10.1021/jp303725j | *J. Phys. Chem. B* 2012, 116, 11635−11645

anionic form, bearing one negative charge per DPPG molecule. In bulk solution, the RBT molecule is mostly in the zwitterionic form at physiological pH, with no net charge. There is a certain contribution of the cationic form of RBT, appointed to be ca. 10% of the total RBT molecules due to the piperidine ring.[9] The molecular structures of the mentioned compounds are shown in Figure 1.

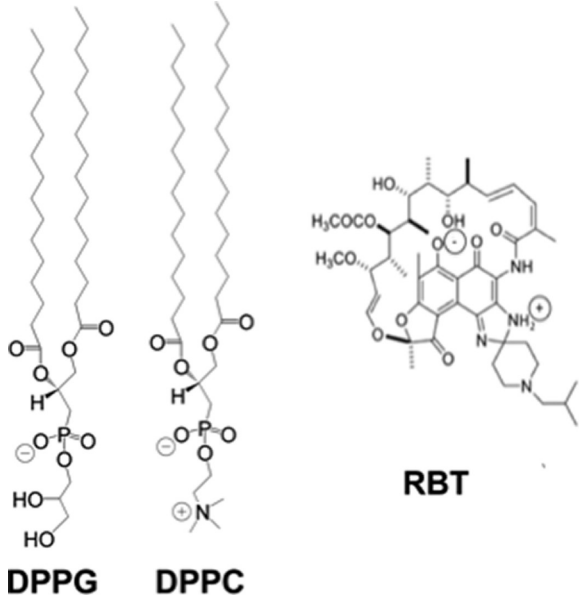

Figure 1. Molecular structures of anionic DPPG, zwitterionic DPPC, and Rifabutin RBT.

To achieve the proposed aim, the effect of the RBT on the phospholipid Langmuir monolayers was studied by a combination of experimental techniques in situ at the air/solution interface. Thermodynamic information was obtained by surface pressure-molecular area isotherms that when associated with Brewster angle microscopy (BAM) allowed recorded images of the monolayer on the micrometer scale. Moreover, UV−vis spectroscopy at the air/solution interface was used for quantifying the amount of RBT at the interface whereas polarization-modulated infrared reflection−absorption spectroscopy (PM-IRRAS) provided information on the methylene and phosphate groups. Computer simulations using a molecular mechanics method were performed to attain additional insight into the interaction between DPPC and RBT molecules with atomic details.

EXPERIMENTAL SECTION

Materials. DPPC and DPPG were purchased as sodium salts from Avanti Lipids, and used as received. RBT was isolated from Mycobutin and purified by column chromatography on silica and was compared with an authentic sample supplied by UpJohn & Pharmacy. The molecular structures of the phospholipids and the RBT are depicted in Figure 1. Chloroform was used as the spreading solvent for dissolving both components. The pure solvents were obtained from Aldrich and used without further purification. Phosphate buffer with a total phosphate concentration of 100 mM at a pH of 7.4 plus 100 mM NaCl was used as a subphase. The subphase containing RBT was composed by the mentioned phosphate buffer with RBT in a final concentration of 0.118 μM. This concentration of the RBT drug was used according to the concentration that has proved to be efficient in vitro, against *M. tuberculosis* and *M. avium*. Moreover, this concentration has proven to be nontoxic against Vero cells, as described in a previous study.[4] Ultrapure water was produced by a Millipore Milli-Q unit, pretreated by a Millipore reverse osmosis system (>18.2 MΩ cm). The subphase temperature was 21 °C. All experiments were performed in a large class 100 clean room.

Methods. Two different models of Nima troughs (Nima Technology, Coventry, England) were used. A Wilhelmy-type dynamometric system using a strip of filter paper was used to monitor the surface pressure. A NIMA 611D Langmuir trough with one moving barrier was used for the measurement of the UV−vis reflection spectra. A NIMA 601 Langmuir trough equipped with two symmetrical barriers was used to record the BAM images. A KSV Langmuir trough was used for measuring the PM-IRRAS spectra. The monolayers were compressed at a speed of ca. 0.1 nm^2 min^{-1} lipid $molecule^{-1}$. UV−visible reflection spectra at normal incidence as the difference in reflectivity (ΔR) of the dye film-covered water surface and the bare surface were obtained with a Nanofilm Surface Analysis Spectrometer (RefSpec^2 supplied by Accurion GmbH, Goettingen, Germany). Images of the film morphology were obtained by Brewster angle microscopy (BAM) with a I-Elli2000 (Accurion GmbH), using a 50 mW Nd:YAG diode laser with a wavelength of 532 nm. The recorded images had a lateral resolution of 2 μm. The image processing procedure included a geometrical correction of the image, as well as a filtering operation to reduce interference fringes and noise. The microscope and the film balance were located on a table with vibration isolation (antivibration system MOD-2 S, Accurion, Goettingen, Germany). PM-IRRAS spectra were recorded using a KSV PMI 550 (KSV NIMA, Espoo, Finland) equipped with an MCT detector. The setup consists of an IR source, a Michelson interferometer and an external reflection unit. The infrared radiation intensity was modulated by the interferometer and polarized with a ZnSe polarizer. The beam was then passed through a ZnSe photoelastic modulator, which modulated it between polarization in the plane of incidence (p) and polarization perpendicular to this plane (s) with a fixed frequency of 100 kHz. The angle of incidence of the infrared beam with respect to the surface normal was 80°. Spectra were recorded with a spectral resolution of 8 cm^{-1} and collected using 3000−6000 scans during 5−10 min. HyperChem 7.51 was used for the molecular mechanics simulations.[12]

Computer Simulations. The un-ionized form of the RBT molecule has been used for the complete set of calculations. The geometry of the DPPC and RBT molecules were optimized using classical molecular mechanics, i.e., MM+ force field, with no partial charges prior to the study of the interactions between those molecules. After the MM+ optimization, the charges were assigned using the PM3 semiempirical method in a single-point fashion. The following step was a second optimization of the molecular geometry using MM+. This procedure was repeated until convergence was achieved. The convergence criteria for geometrical optimization was 0.001 kcal/(Å·mol). A similar method of assigning partial charges was used elsewhere.[13,14] The procedure for studying the interactions between the DPPC and RBT molecules is described as follows: the position of the RBT and DPPC molecules were fixed. The complex geometry was optimized using the MM + force field with electrostatic atomic charge, including no cutoffs. The Polak−Robiere

method was used for minimizing the energy by varying the geometry of the complex. The convergence criteria was 0.002 kcal/(Å mol).

RESULTS AND DISCUSSION

Surface Pressure–Molecular Area (π–A) Isotherms. The surface pressure-molecular area (π–A) isotherms of the DPPC monolayer, both with and without Rifabutin (RBT) on the phosphate buffer subphase, are shown in Figure 2. A clear

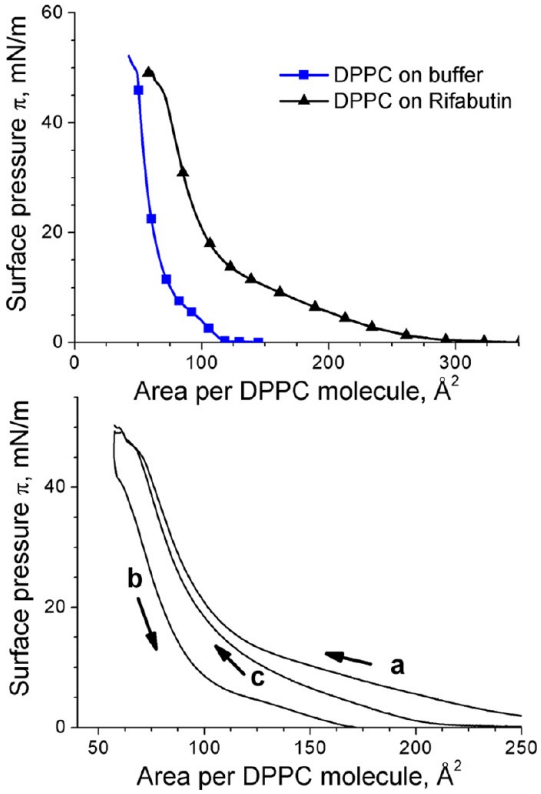

Figure 2. Top: Surface pressure-molecular area (π–A) isotherms for the DPPC monolayer on phosphate buffer (blue squares) and on phosphate buffer containing 0.12 μM of RBT (black triangles). The sampling of the surface pressure was continuous. Symbols are included for clarity. Bottom: surface pressure-molecular area isotherm cycles of the DPPC monolayer on the subphase containing RBT. a: first compression, b: decompression, and c: second compression.

expansion of the π-A isotherm is observed when RBT is present in the subphase, indicating the presence of the drug molecules at the DPPC monolayer. This expansion is still significant even at later stages of compression of the DPPC monolayer, i.e., at low values of molecular area. The liquid expanded-liquid condensed (LE-LC) transition might take place simultaneously with a certain rearrangement of RBT and DPPC molecules in the region of molecular areas between 125 and 250 Å^2 per DPPC molecule, although the detailed physical phenomenon can not be deduced from the π–A isotherm. The expansion of the molecular area in the DPPC monolayer provoked by the presence of RBT is ca. 160 Å^2 per DPPC molecule at low stages of compression of ca. 2 mN/m. The expansion of the π–A isotherm of DPPC at a surface pressure of 30 mN/m is reduced to ca. 30 Å^2 per DPPC molecule.

The stability of the RBT molecules attached to the DPPC monolayer has been tested by performing two subsequent compression π–A isotherms of the DPPC monolayer with Rifabutin in the subphase (Figure 2). A certain degree of hysteresis is observed with the decompression of the DPPC monolayer. This hysteresis might be ascribed to either an irreversible conformational change of the DPPC and RBT molecules or to a loss of RBT molecules from the DPPC monolayer. The second compression π–A isotherm shows a slight deviation from the first π–A isotherm at high values of surface area (Figure 2). However, with compression of the DPPC monolayer, the π–A isotherms for the first and second compressions overlap, indicating the similarity of the final state of the DPPC monolayer in both compressions. Quantitative insight into the amount of RBT present at the DPPC monolayer with the compression and decompression processes are attained with UV–vis reflection spectroscopy, as discussed below.

A mixed monolayer formed by the zwitterionic DPPC and the anionic DPPG phospholipids in a molar ratio DPPC:DPPG 9:1 has been used as a model for the lung surfactant monolayer. This molar ratio has been chosen to mimic the pulmonary surfactant, in which ca. 5–10% of the total content of lipids are anionic PG lipids.[5] Moreover, the incorporation of a certain degree of negative charge in the mixed phospholipid monolayer might offer information on the relevance of electrostatic interactions between RBT and phospholipids. The π–A isotherms of the mixed monolayer DPPC:DPPG on the phosphate buffer subphase, both with and without RBT, are shown in the Figure 3. Note that in this case of a mixed monolayer, the molecular area is expressed as the mean molecular area per phospholipid molecule, i.e., the DPPC and DPPG molecules are considered equivalent.

A similar situation to the one previously observed for the pure DPPC monolayer is achieved in the case of a mixed monolayer. The expansion in the molecular area when comparing the mixed monolayer DPPC:DPPG 9:1 in the presence and absence of RBT is ca. 160 Å^2 per lipid molecule at low stages of compression, as in the previous case of a pure DPPC monolayer. The expansion of the π–A isotherm of the mixed monolayer DPPC:DPPG at a surface pressure of 30 mN/m is slightly larger than for the DPPC case, reaching a value of ca. 40 Å^2 per phospholipid molecule.

The stability of the attachment of the RBT molecules to the lipids composing the mixed monolayer has been tested by two-cycle compression π–A isotherms of the mixed monolayer DPPC:DPPG 9:1 with Rifabutin in the subphase, as shown in Figure 3. A certain hysteresis is observed during the decompression process. An almost complete recovery of the π–A isotherm for the second compression is observed for high values of surface pressure, pointing to a persistent presence of the RBT in the mixed monolayer DPPC:DPPG 9:1. Additional information concerning the amount of RBT is provided by UV–vis reflection spectroscopy, as discussed below.

Brewster Angle Microscopy. Brewster angle microscopy (BAM) allows the direct visualization of the Langmuir monolayer at micrometer dimensions.[15] Figure 4 shows BAM images acquired during the compression of a DPPC monolayer on a phosphate buffer subphase, both with and without RBT. The morphology of the DPPC monolayer is described in the literature with deeper detail.[16] Briefly, during the first-order transition in the π–A isotherm the formation and growth of bright domains is observed. These bright domains correspond to aggregates of phospholipid molecules in a more condensed state (LC) than the phospholipid molecules in the surrounding media (LE). With further compression of the DPPC

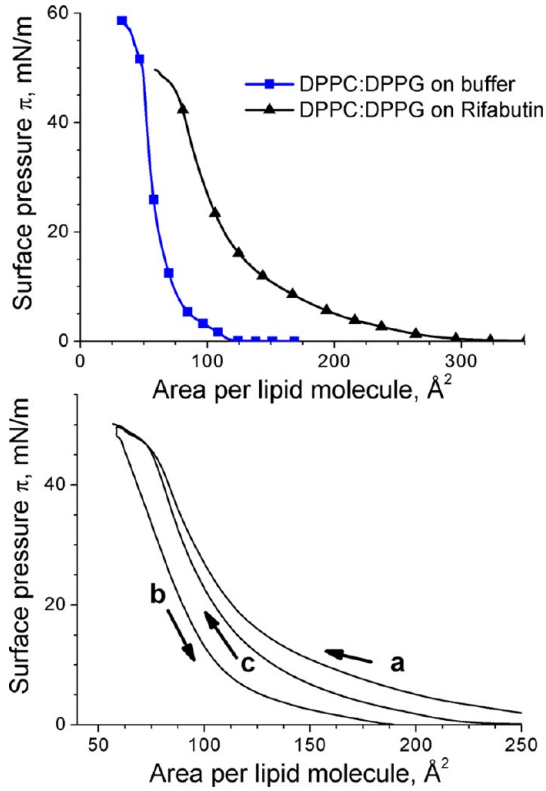

Figure 3. Top: Surface pressure-molecular area (π–A) isotherms for the mixed monolayer DPPC:DPPG 9:1 on phosphate buffer (blue squares) and on phosphate buffer containing 0.12 μM of RBT (black triangles). The sampling of the surface pressure was continuous. Symbols are included for clarity. Bottom: Surface pressure-molecular area isotherm cycles of the mixed monolayer DPPC:DPPG 9:1 on the subphase containing Rifabutin. a: first compression, b: decompression, and c: second compression.

monolayer, the domains grow and coalesce. In the final stage of compression, a bright homogeneous monolayer is observed.

When RBT is incorporated in the subphase, clear changes in the morphology of the DPPC monolayer are observed. At large values of molecular area, i.e., a highly expanded state of the DPPC monolayer small bright points, a few micrometers in size, are observed. These bright points might correspond to aggregates of RBT, although the chemical composition can not be unambiguously deduced from the BAM images. With compression of the DPPC monolayer, the domains corresponding to DPPC molecules in the LC phase appear. However, in this case almost all the LC domains are formed around the bright domains in a yolk-egg white fashion. The bright domains are already present at large values of molecular area. It is tempting to ascribe this phenomenon to the growth of DPPC domains in the LC state around aggregates formed mainly by DPPC/RBT complexes. In this scenario, the DPPC/RBT complex aggregates would serve as nuclei. A similar phenomenon has been described by Deng et al., in which an inorganic/organic hybrid molecule, i.e., a oligomeric silsesquioxane formed well-defined mono and multilayer at the air/water interface.[17−19] In the case of the silsesquioxane, the origin of the domains is related with the formation of multilayers. Remarkably, the authors use different spreading conditions, e.g., spreading on hot water and then cooling, to avoid the aggregation of the silsesquioxane molecules prior to compression.

This possibility is examined in deeper detail below, where computational simulations show that the DPPC molecule can interact with the RBT molecule forming a noncovalent inclusion complex. With further compression of the DPPC monolayer, the domains become closer to each other. In contrast to the pure DPPC monolayer, there is no total coalescence of the LC domains in the presence of RBT. When the drug RBT is present in the subphase, the bright domains in the DPPC monolayer form an inhomogeneous monolayer at high values of surface pressure. The nonhomogeneity of the monolayer might be provoked by an interfering effect of the RBT against the intermolecular DPPC attractive interactions, which would agree with the hypothesis of an inclusion complex RBT-DPPC. In this highly compressed state, the brightness of the picture is quite high, indicating a thick monolayer.

The BAM pictures recorded during compression of the mixed monolayer DPPC:DPPG 9:1 with RBT in the phosphate buffer subphase are shown in Figure 4. The domains appear smaller and with slightly rounder shapes than in the pure DPPC monolayer. This modification of the domains indicates a more significant effect of the line tension.[20] There is also a fraction of the monolayer displaying short quasiellipsoidal bright structures, which might correspond to DPPG lipid, as observed in the pure DPPG monolayer.[21]

Bright small domains and large fiber-like structures appear in the LE phase of the monolayer at ca. 7 mN/m. The bright domains show the same yolk-egg white appearance as in the pure DPPC monolayer. These domains exist along the entire isotherm. The domains display a small growth with compression of the monolayer. There is no coalescence of the domains even at a large degree of compression. The fiber-like structures grow in size with compression of the monolayer, reaching the form of elongated strips with a length of ca. 10–100 μm. There is apparently no interaction between the two types of domains. We hypothesize that the stripes might be composed of aggregates of lipids and RBT with a nondefined stoichiometry.

A magnified view of selected BAM pictures is shown in Figure 5. The coexistence of the brighter regions with the domains usually observed for lipids in a LC phase indicates the occurrence of aggregates of RBT in the polar head region of the phospholipids.[22] On the other hand, the domains are due to the arrangement of the alkyl chains of the phospholipids. The aggregation of the RBT molecules might be mediated by the polar head of the phospholipids. The interaction of RBT molecules with the polar head groups of the phospholipids is consistent with the absence of perturbation of the alkyl chains by RBT, as shown hereafter by PM-IRRAS.

UV–vis Reflection Spectroscopy. The expansion of the π–A isotherms and the BAM pictures offer direct proof for the existence of RBT in the phospholipid monolayer. Quantitative insight into the actual amount of RBT at the air/solution interface is highly desirable as is monitoring the impact of compression and decompression on the presence of RBT at the air/solution interface. To this end, UV–vis reflection spectroscopy at the air/solution interface is a highly valuable tool. The UV–vis reflection spectroscopy is exclusively sensitive to the chromophores located at the air/water interface, therefore being most useful for the in situ characterization of the Langmuir monolayers.[23]

The UV–vis reflection spectra of the DPPC monolayer at different stages of compression of the DPPC monolayer with RBT in the subphase are shown in Figure 6. The bulk UV–vis

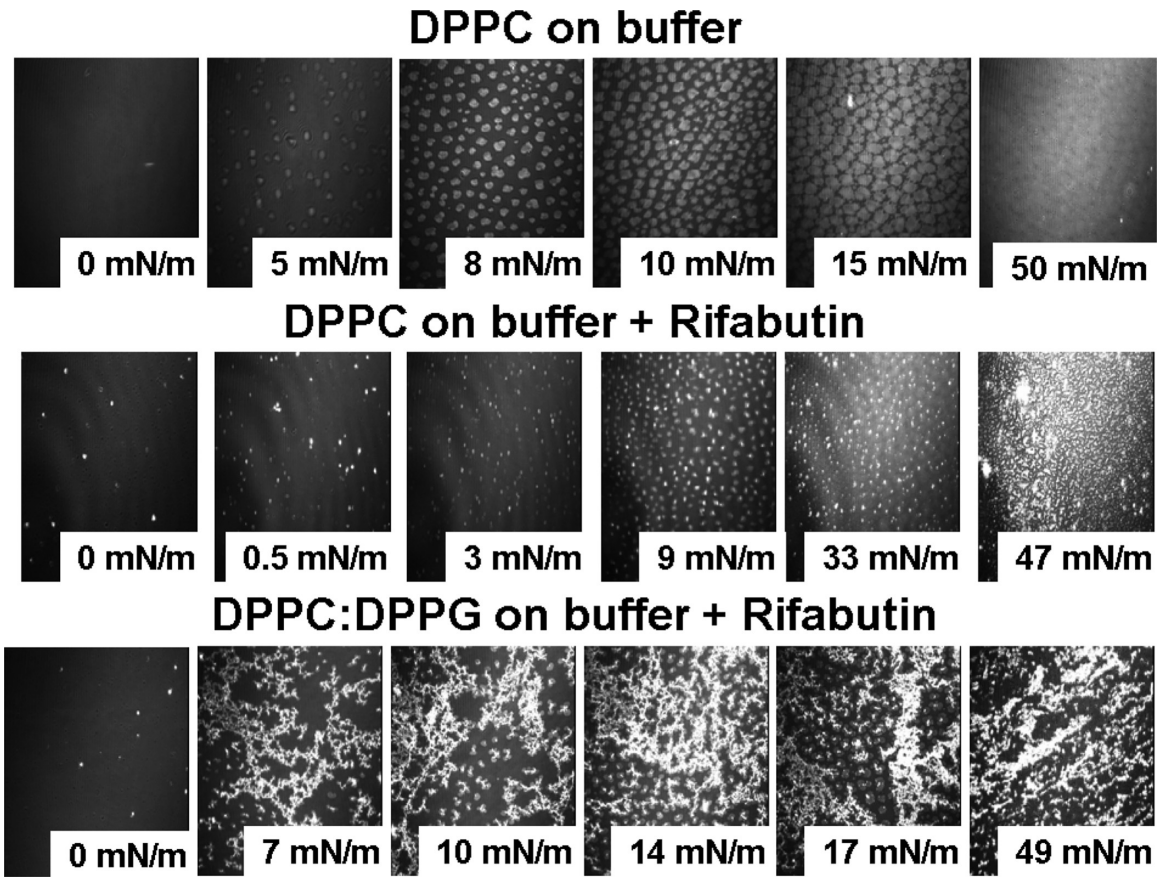

Figure 4. Brewster angle microscopy pictures of (top) a DPPC monolayer on a phosphate buffer subphase, (middle) a DPPC monolayer on a phosphate buffer containing 0.12 μM of RBT subphase, and (bottom) and a mixed DPPC:DPPG 9:1 monolayer on a phosphate buffer containing 0.12 μM of RBT subphase. Surface pressures for each image are indicated on the images, which have widths of 430 μm.

spectrum of RBT is included for comparison. The bulk UV−vis spectrum shows two main peaks centered at ca. 280 and 325 nm, as well as a shoulder at ca. 530 nm. The position of the peaks in the reflection spectra are clearly modified, indicating the presence of different states of aggregation of the RBT molecules at the air/solution interface than that of the bulk solution. Therefore, the maxima and minima of the UV−vis spectra are not clearly displayed. The intensity of the reflection signal increases with the compression of the DPPC monolayer. This increase indicates that the air/solution interface is enriched in RBT with compression of the lipid monolayer. The intensity of reflection is proportional to the relative amount of RBT located at the air/solution interface. The UV−vis reflection spectra have been integrated, and the integral values of the UV−vis reflection spectra obtained during the two π−A compression isotherms are shown in Figure 6. Note that the reference spectrum is acquired using the RBT subphase with no monolayer of phospholipid. Therefore, the UV−vis reflection signal from adsorbed molecules of RBT at the interface is neglected. Almost all of the integral coming from surface molecules comes from wavelengths below 300 nm. Control experiments with pure DPPC, pure DPPG, and DPPC:DPPG monolayers on phosphate buffer subphase without RBT were performed, showing the absence of a significant UV−vis reflection signal in all cases. The integral values are displayed as a function of the molecular area of the DPPC for direct comparison of the UV−vis reflection signal with the π−A isotherms in Figure 2. The amount of RBT in contact with the DPPC monolayer at the air/solution interface increases almost linearly with compression of the monolayer. The surface concentration of RBT molecules reaches the maximum value for the most compressed state of the DPPC monolayer. Remarkably, with the second compression of the DPPC monolayer a certain degree of hysteresis appears. The hysteresis is observed only at large values of molecular areas. The amount of RBT molecules at the air/solution interface is fully recovered at high stages of compression of the DPPC monolayer. The total recovery of RBT might indicate the reversibility of the maximum amount of the RBT molecules at the DPPC monolayer after the "squeezing-out" of the excess RBT molecules after compression of the monolayer. This reversible state of as maximum surface concentration of RBT in contact with the polar heads of the lung surfactants might occur at the lungs, where the successive breathing cycles expand and compress the lung surfactant monolayer.

The UV−vis spectra of the mixed monolayer DPPC:DPPG 9:1 in the presence of RBT are shown in Figure 7. The UV−vis reflection spectra for the DPPC/DPPG monolayer appear slightly noisier than those of the pure DPPC monolayer. The drift of the UV−vis reflection signal is a common experimental feature, especially when considering a broad range of wavelength, i.e., 250 to 700 nm. This drift is usually related with a certain mismatch between the reference and the sample spectra, i.e., the bare air/solution interface and the Langmuir monolayer, respectively. In the case of the UV−vis reflection spectra presented in the Figure 7, the drift in the long wavelength region is not considered significant for the spectral region of interest that is mainly the UV region. The significant

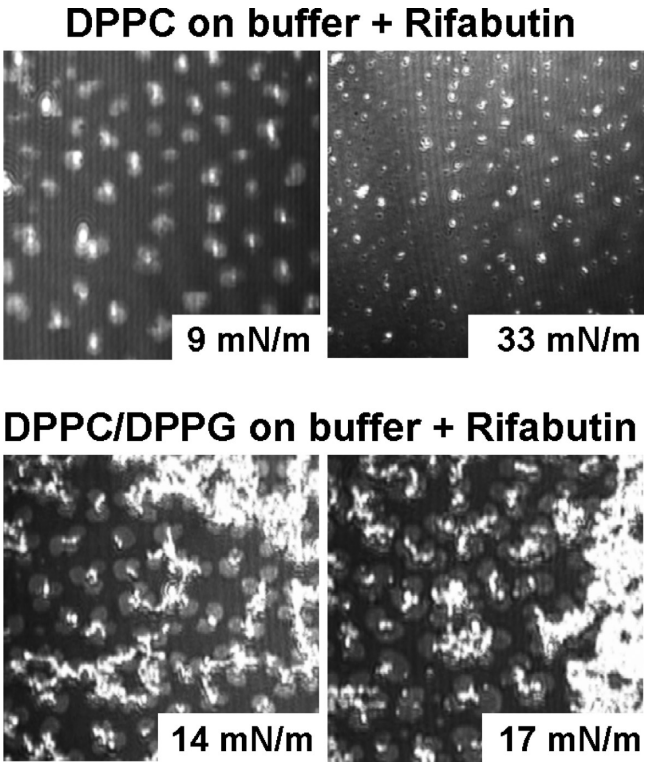

Figure 5. Magnified Brewster angle microscopy pictures. (Top) A DPPC monolayer and (bottom) a mixed DPPC:DPPG 9:1 monolayer on a phosphate buffer subphase containing 0.12 μM of RBT subphase. Surface pressures for each image are indicated on the images, which have widths of ca. 200 μm.

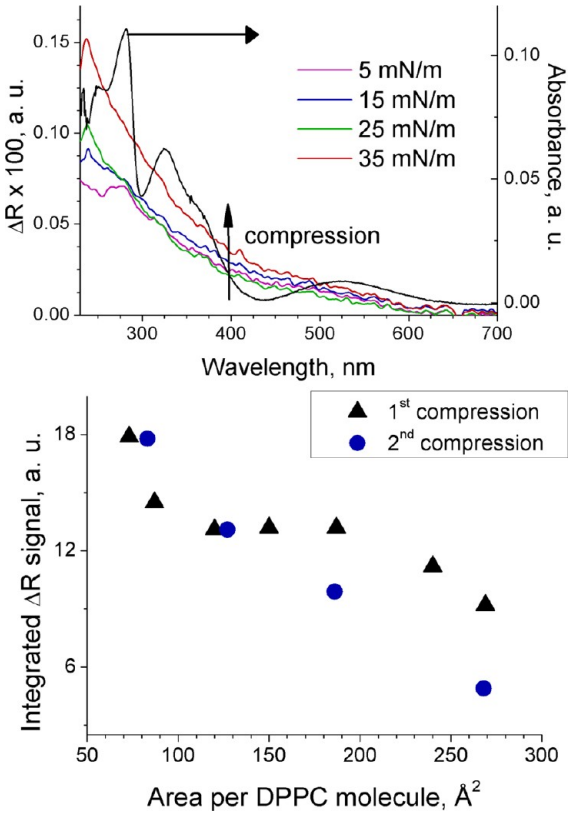

Figure 6. Top: UV–vis reflection spectra of the DPPC monolayer on a phosphate buffer containing 0.12 μM of RBT subphase at different values of surface pressure. The UV–vis spectrum of RBT in bulk solution (2×10^{-6} M in phosphate buffer solution) is included for comparison. Bottom: Integral values of the complete UV–vis reflection spectra at different values of molecular area of DPPC obtained during two successive compression π–A isotherms. Error is within experimental deviation of ca. 10%.

UV–vis reflection signal at 0 mN/m indicates the adsorption of a given amount of RBT molecules at the DPPC:DPPG 9:1 mixed monolayer prior to compression of the monolayer.

The introduction of the anionic DPPG phospholipid into the mixed monolayer leads to a reduced amount of RBT molecules at the air/solution interface, as shown by the smaller integral values of the UV–vis reflection spectra than those of the DPPC case. In the case of a mixed monolayer DPPC:DPPG 9:1, the saturation state is almost reached since ca. 250 Å^2 per phospholipid molecule. Further compression of the mixed DPPC:DPPG 9:1 monolayer leads to a small albeit significant increase of the amount of RBT at the air/solution interface. The reversible state of the maximum amount of RBT at the mixed DPPC:DPPG 9:1 monolayer for the two compression cycles are almost equivalent. Thus, the UV–vis reflection spectroscopy data might point to a slightly less favorable interaction between the anionic DPPG and the RBT molecules than between the zwitterionic DPPC and the RBT molecules for a highly compressed monolayer, taking into account exclusively the absolute values of UV–vis reflection signal. The RBT molecule is mostly in zwitterionic form with a slight contribution of cations, ca. 10%, at a pH value of 7.4 as used in the subphase.[9] Therefore, the electrostatic interactions do not contribute to a large extent to the RBT-phospholipid interactions. On the contrary, the polar headgroup of the phospholipids seems to play a significant role in the interactions between the phospholipid and RBT molecules via the formation of a noncovalent complex. Computer simulations confirm the relevance of the polar headgroup of the lipids, as described below.

The numerical values of the integral of the UV–vis reflection spectra are normalized using $\Delta R_{norm} = \Delta R \times$ lipid area,[24] so that the value of lipid area in this case is not fixed, i.e., each ΔR value is multiplied by the value of lipid area at which the UV–vis reflection spectrum was recorded. The variation of the normalized value of the integral with the compression of the monolayer is indicative of the relative changes of the surface concentration of the chromophore per lipid molecule, i.e., the variation of the surface concentration of the RBT molecules with the area per lipid. For the case of the presence of RBT at the air/solution interface exclusively forming a stable DPPC/RBT complex no variation of the normalized integral of the UV–vis reflection signal with the compression of the monolayer is expected. In other words, the intensity of the signal ΔR would vary in the same magnitude as the area per lipid molecule, thereby ΔR_{norm} being constant. On the other hand, for a "squeezing-out" of the RBT molecules from the air/solution interface to the bulk solution, a diminution of the normalized integral of the UV–vis reflection signal with the compression of the monolayer is expected. Figure 8 shows the normalized integral of the UV–vis reflection signal for the two compression isotherms of the DPPC and DPPC:DPPG monolayers on a RBT solution subphase. The results for both lipid monolayers are similar, indicating a similar mechanism of adsorption of RBT molecules at the lipid monolayer/solution interface. For the first compression, the

dx.doi.org/10.1021/jp303725j | J. Phys. Chem. B 2012, 116, 11635–11645

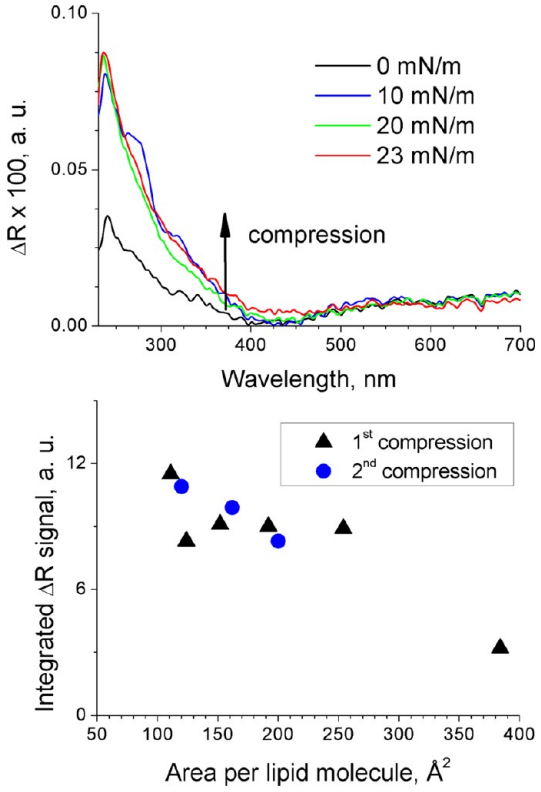

Figure 7. Top: UV−vis reflection spectra of the DPPC:DPPG 9:1 mixed monolayer on a phosphate buffer containing 0.12 μM of RBT subphase at different values of surface pressure. Bottom: Integral values of the complete UV−vis reflection spectra at different values of mean molecular area of phospholipid obtained during two successive compression π−A isotherms. Error is within experimental deviation of ca. 10%.

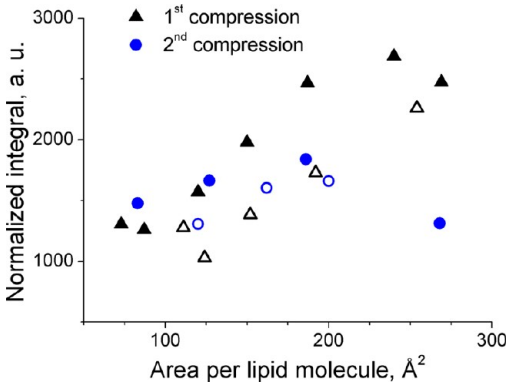

Figure 8. Normalized integral value of the UV−vis reflection spectra of both DPPC monolayer and DPPC:DPPG 9:1 mixed monolayer on a phosphate buffer containing 0.12 μM of RBT subphase. Full symbols: DPPC monolayer. Empty symbols: Mixed DPPC:DPPG mixed monolayer. Triangles: First compression. Circles: Second compression. The UV−vis reflection spectra were obtained during two compression π−A isotherms.

normalized integral diminishes with the compression of the lipid monolayer, indicating the loss of a significant amount of RBT per lipid molecule from the lipid monolayer/solution interface. On the contrary, during the second compression the normalized integral is approximately constant. Therefore, the ratio between the RBT and DPPC molecules at the air/solution interface is constant. This behavior is indicative of the formation of a noncovalent complex comprising RBT and lipid molecules during the first compression isotherm. This complex is stable, thus leading to a constant amount of RBT molecules at the lipid monolayer/solution interface in the second compression isotherm. As previously commented, this complex is attributed to an inclusion complex. This possibility is discussed in detail hereafter with respect to computer simulations and PM-IRRAS measurements.

Computer Simulations. The experimental data presented above suggest an interaction between the RBT and the phospholipids concerning mainly the polar headgroup of the phospholipids. Computer simulations have been performed using a simple model of one DPPC molecule and one RBT molecule in vacuo. In spite of the simplicity of the model, the simulated structures are consistent with the experimental results; therefore the simulations performed herein are viewed as complementary to the experimental findings. We should remark that we use the computational simulations to test the feasibility of the formation of the DPPC/RBT inclusion complex. The simulations performed herein are not intended to offer a direct proof of the formation of the DPPC/RBT inclusion complex.

In the seminal work of Casey and Whitlock, the different conformations of the Rifamycin molecule, an analogue to the RBT molecule, were analyzed.[25] The Rifamycin molecule is assumed to form an inclusion complex with a hydrophobic group, e.g., a tyrosine residue in bulk solution using water as a solvent. However, no direct experimental proof of the formation of an inclusion complex was described in the cited paper.

The situation described for Rifamycin in bulk water can not be directly extrapolated to RBT at the air/solution interface due to the spatial constraints. On the other hand, given the similarities between the molecular structures of Rifamycin and Rifabutin molecules, the formation of an inclusion complex with RBT as a host is worthy to be examined.

The computational procedure for analyzing the feasibility of the formation of the DPPC/RBT inclusion complex is as follows: The position of the DPPC lipid molecule was fixed. The DPPC polar group is considered for simplicity as the group of atoms N−C−C−O−P. The main axis of the polar headgroup is defined as the line connecting the N and P atoms. The RBT molecule is placed at different positions around the polar headgroup, therefore generating different starting configurations. The central position of the RBT cavity is located around the polar headgroup of the DPPC lipid in all cases.

A systematic study on the effect of the initial position of the RBT molecule in the optimized molecular geometry of the inclusion complex has been carried out. The initial displacement of the RBT molecule is defined as the distance between the central part of the RBT cavity and the N atom of the DPPC polar headgroup. The initial displacement was varied over a range of 5 Å, in steps of 1 Å for generating the different starting configurations. The total energy of the DPPC/RBT system was then evaluated. Please note that this method is not a molecular dynamics procedure, and water molecules are not included, therefore the effect of solvation of the DPPC headgroups is not studied. The molecular dynamics simulations of the DPPC/RBT inclusion complex lead to a significant change in the geometry of the alkyl chains of the lipids. The alkyl chains collapse on themselves after a few picoseconds. Remarkably, in no case of collapse of the alkyl chains the breakup of the

dx.doi.org/10.1021/jp303725j | J. Phys. Chem. B 2012, 116, 11635−11645

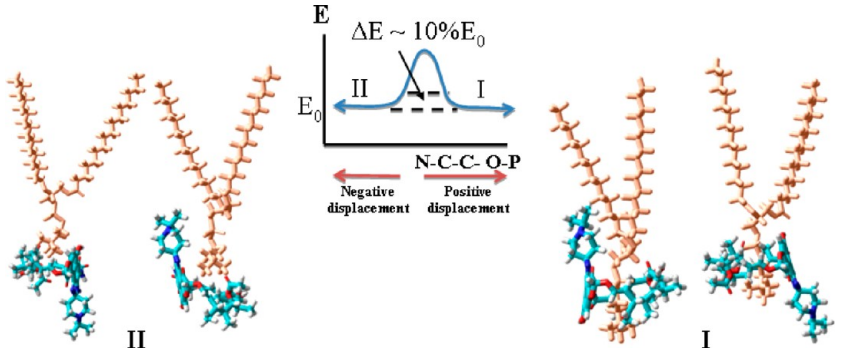

Figure 9. Left and right: Snapshots of the computer simulations of the DPPC and RBT molecules, and the change of the calculated total energy as a function of the initial configuration. Center: Scheme depicting the relative energy of stabilization gained by forming the DPPC/RBT inclusion complex. *Y* axis is energy. Brown: DPPC phospholipid molecule. The RBT molecules are displayed in white (hydrogen), light blue (carbon), red (oxygen), and deep blue (nitrogen).

inclusion complex has been observed. On the other hand, the molecular mechanics method used herein is able to find the closest minimum of energy to the starting point. Two trends of the calculated energy with the relative initial position of the RBT molecule around the DPPC molecule have been observed: for a positive value of the initial position of the RBT molecule, i.e., the RBT molecule moving deeper into the DPPC headgroup, the optimization procedure results in the formation of a DPPC/RBT inclusion complex. The RBT ring plane is displaced from the initial position of the O atom of the DPPC polar headgroup by a distance of ca. 3.6 Å from the N atom in the minimum of energy. The N atom of the DPPC headgroup is used as a reference position, i.e., zero position. The positive displacement is defined as the displacement of the ring plane of the RBT molecule displaced toward the P atom. On the other hand, the negative displacement consists in a movement of the ring plane of the RBT molecule displaced toward the alkyl chain region. For a negative value of the initial position of the RBT molecule, the optimization procedure leads to the formation of a DPPC/RBT pair, in which the interaction between the DPPC and RBT molecules is non specific. For both cases, the calculated energy of the system comprising the DPPC and RBT molecules is approximately the same, i.e., less than a 10% difference. Remarkably, both interacting combinations of DPPC and RBT, with and without forming the inclusion complex, are more stable than the DPPC and RBT molecules with no interaction by a factor of ca. 4. In other words, the computed energy for the set of one DPPC molecule and one RBT molecule is ca. 4 times lower in the case of an interaction between the DPPC and RBT molecules.

These computational results point to the formation of the two types of DPPC/RBT pairs at the air/water interface: inclusion complex and non specific interaction. The computational results are in agreement with the experimental results, in which we observe the enrichment of the air/solution interface in RBT molecules. Remarkably, a certain fraction of the RBT molecules is expelled out from the DPPC lipid monolayer after the first compression. The RBT molecules expelled out in this way might be those with a non specific interaction DPPC/RBT, whereas those RBT molecules forming the DPPC/RBT inclusion complex stay attached to the DPPC lipid monolayer even after the compression of the Langmuir monolayer.

Therefore, there is a stabilization of the global system by the interaction between the DPPC and RBT molecules. The driving force, as well as the stabilization mechanism, for the DPPC/RBT inclusion complex, is discussed below. There is certain energy of activation for modifying the interaction mode of the DPPC and RBT molecules. The DPPC/RBT inclusion complex might be formed during the spreading of the DPPC lipid layer, or during the compression. The stabilization of the DPPC/RBT system by the formation of the inclusion complex is summarized in the Figure 9.

The formation of two intermolecular hydrogen bonds with an average length of 2.2 ± 0.2 Å is observed in the DPPC/RBT complex. The H-bonds are formed between the two −OH groups of the ansa bridge for the RBT molecule, and the negatively charged oxygen of the phosphate group for the DPPC molecule. The driving force for the formation of the DPPC/RBT inclusion complex is ascribed to the formation of the intermolecular H-bonds. The formation of these H-bonds is exclusive for the DPPC/RBT inclusion complex, not being detected in the case of alternative configurations. The intermolecular H-bonds are shown in the Figure 10.

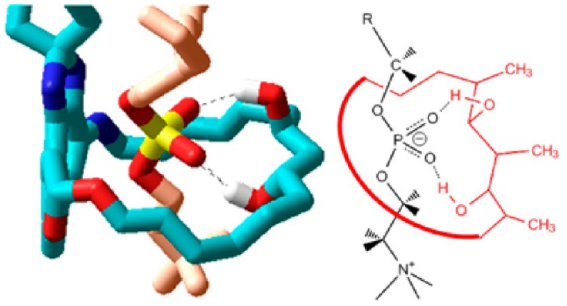

Figure 10. Left: Snapshots of the simulation of the DPPC:RBT inclusion complexes. The intermolecular H-bonds are displayed as dashed black lines. Methyl groups are not displayed for clarity. Right: Scheme depicting the atoms involved in the intermolecular H-bonds. Brown: DPPC phospholipid molecule, with red (oxygen) and yellow (phosphorus). The RBT molecule is displayed in white (hydrogen), light blue (carbon), red (oxygen), and deep blue (nitrogen).

Additionally, the conformational configuration of the RBT molecule in the DPPC/RBT inclusion complex might be relevant. In the case of the DPPC/RBT inclusion complex, the central cavity of the RBT molecule is located around the oxygen atoms of the DPPC headgroup. Given the sequence of atoms $-N-CH_2-CH_2-O-P-$, the smaller volume of the headgroup is found around the oxygen connecting the phosphorus atom with the methylene groups. The steric

dx.doi.org/10.1021/jp303725j | J. Phys. Chem. B 2012, 116, 11635−11645

hindrance is minimized at this point, and the coupling of the RBT cavity with the DPPC lipid is favored.

The formation of the DPPC/RBT inclusion complex is feasible. The formation of the DPPC/RBT inclusion complex requires a certain value of activation energy. The formation of a nonspecific coupling, i.e., noninclusion complex, between the DPPC and the RBT molecules does not require such an energy, thereby being more labile.

These two types of conformations for the pair formed by the DPPC and RBT molecules are consistent with the experimental results at the air/solution interface presented herein. As commented, a significant loss of RBT molecules from the air/solution interface is observed during the first compression cycle. On the contrary, the number of RBT molecules is approximately constant during the second compression cycle. This behavior might be interpreted as follows. Initially, the DPPC lipid monolayer is spread over the air/solution interface. A certain number of RBT molecules are then adsorbed from the bulk solution onto the DPPC lipid monolayer. Two main types of interactions between the DPPC and RBT molecules are expected: the DPPC/RBT inclusion complex and a nonspecific interaction between the DPPC polar headgroup and the RBT molecule. With the first compression cycle, the adsorbed RBT molecules that do not form inclusion complexes are likely to be expelled from the air/solution interface due to molecular crowding, given that the area occupied per DPPC molecule is smaller than that of the RBT molecule. On the other hand, the adsorbed RBT molecules included in the DPPC/RBT inclusion complex are less likely to be expelled from the air/solution interface, given that the breaking of the DPPC/RBT inclusion complex requires a certain activation energy. Moreover, the area occupied per unit of DPPC/RBT inclusion complex is only slightly larger than the area per DPPC lipid molecule. This small increase of the DPPC lipid area by the presence of RBT in the DPPC/RBT inclusion complex should not disturb to a large extent the arrangement of the DPPC lipids in the Langmuir monolayer. A semi-quantitative calculation on the increment of molecular area per DPPC molecule provoked by the RBT can be performed, considering the RBT a 2D disk. According to the simulations, the diameter of the RBT molecule can reach a value of ca. 7 Å. Thus, the expansion of the $\pi-A$ isotherm of DPPC in case of the formation of an inclusion complex with RBT might lead to an expansion of ca. 50 Å^2. As commented previously (Figure 2), the experimental value of expansion of the $\pi-A$ isotherm of DPPC at high stages of compression is ca. 40 Å^2, in approximate agreement with the previously calculated value. The interaction between the alkyl chains of the DPPC lipids and the formation of the domains would occur in the case of a DPPC/RBT inclusion complex, as experimentally observed.

Therefore, the formation of an inclusion complex with stoichiometry DPPC:RBT 1:1 is plausible, given the good agreement of the computational and experimental data. However, we would like to remark that we could not find direct proof of the existence of the DPPC/RBT inclusion complex rather than the proposed model and the consistency between the computational model and the experimental findings.

Polarization-Modulated Infrared Reflection Absorption Spectroscopy. PM-IRRAS allows monitoring of the vibrational spectra of the molecules present at the air/solution interface during the compression process of the $\pi-A$ isotherm. The methylene vibrations are of special interest, being the symmetric $\nu_s(CH_2)$ and antisymmetric $\nu_{as}(CH_2)$ stretching modes for monitoring the aggregation state of the hydrocarbon chains.[26] The PM-IRRAS spectra for the DPPC and the DPPC:DPPG 9:1 monolayers in the presence of RBT in the subphase are shown in Figure 11. A control experiment of a pure DPPC monolayer on a pure water subphase has been included for comparison. The DPPC:DPPG 9:1 mixed monolayer does not show any significant variation with respect to the pure DPPC monolayer, probably due to the relatively small amount of DPPG present in the mixture.

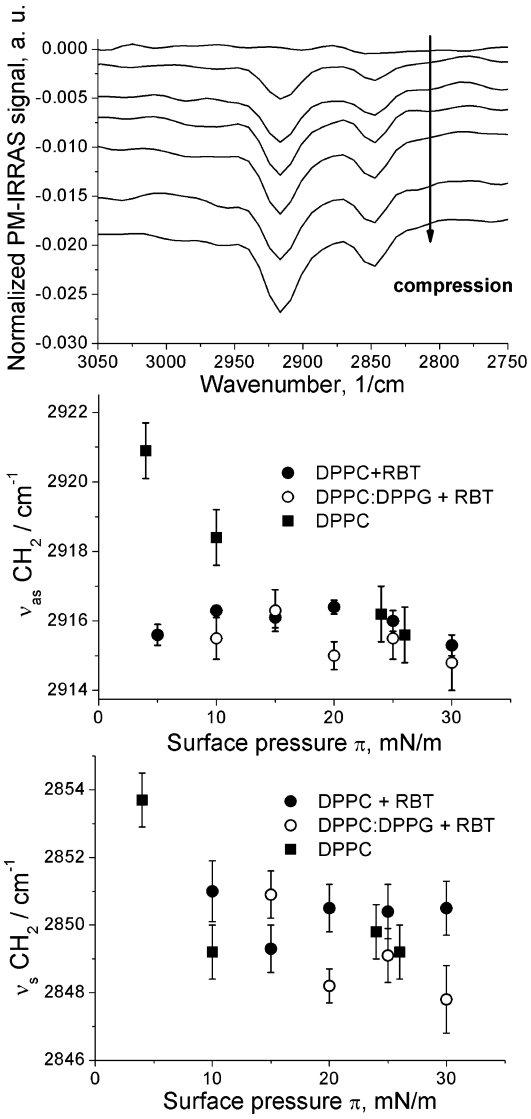

Figure 11. PM-IRRAS spectra of the methylene stretching region of a DPPC (black circles) and DPPC:DPPG 9:1 (empty circles) monolayers on a phosphate buffer containing 0.12 μM of RBT subphase recorded at different surface pressures. A control experiment of a pure DPPC monolayer (black squares) on pure water subphase is included for comparison. (Top) Evolution of the spectra of a DPPC monolayer on a phosphate buffer containing 0.12 μM of RBT subphase with the compression of the monolayer. The spectra are shifted 0.004 each for clarity. (Middle) Wavenumber values of the asymmetric methylene stretching mode with the applied surface pressure. (Bottom) Wavenumber values of the symmetric methylene stretching mode with the applied surface pressure.

dx.doi.org/10.1021/jp303725j | J. Phys. Chem. B 2012, 116, 11635−11645

The $\nu_s(CH_2)$ and $\nu_{as}(CH_2)$ bands are located at ca. 2850 and ca. 2916 cm^{-1}, respectively. These wavenumbers are characteristic from a condensed state of the alkyl chains, therefore indicating a tight packing of the hydrocarbon chains of the DPPC phospholipid molecules. The variation of the methylene stretching modes to lower values with compression of the monolayer is expected, as the alkyl chains become arranged in a more tight state, indicating a phase change.[27] Herein, the wavenumber of the methylene stretching modes are almost constant with the increase of surface pressure for both DPPC and DPPC:DPPG monolayers in presence of RBT. Therefore, we conclude the formation of a DPPC/RBT inclusion complex, as the existence of this complex leads to the observed experimental results, given that the RBT molecule adds eight methylene groups to the complex. The signal arising exclusively from the methylene groups of the phospholipids can not be distinguished from the PM-IRRAS spectra. According to the surface selection rules, the negative sign of the bands indicates a parallel orientation of the transition moment of the methylene groups with respect to the air/solution interface plane, which is consistent with an upright orientation of the alkyl chains.[28] Given a negative contribution of the methylene groups of the RBT molecule, this contribution would indicate an upright orientation of most of these methylene groups. Therefore, the impact of the formation of the inclusion complex in the physical state of the alkyl chain of the phospholipids could not be followed. On the other hand, these results support the idea of the formation of an inclusion complex DPPC:RBT, thus enriching the air/solution interface in methylene content.

In the case of the formation of an inclusion complex between the DPPC and the RBT molecules, a significant impact on the infrared spectrum of the phosphate moiety corresponding to the DPPC lipid is expected. Figure 12 shows the phosphate region of the PM-IRRAS of a DPPC monolayer on a phosphate buffer in presence and absence of RBT. The main band corresponds to the asymmetric stretching mode of PO_2^- group, located at 1252 cm^{-1} in the absence of RBT, and located at 1257 cm^{-1} in presence of RBT.[29] Remarkably, there is an inversion of the sign of this phosphate band, indicating a change in the orientation of the transition moment of the PO_2^- group with respect to the air/solution interface.[30] The phosphate band changes from a negative to a positive sign in the case of the absence and presence of RBT in the subphase, respectively. The change of sign for the PM-IRRAS signal indicates a relative change of orientation of the transition moment with respect to the air/solution interface. This change in conformation is induced by the RBT molecule. The RBT molecule in the DPPC/RBT inclusion complex constrains the conformational freedom of the phosphate group, restraining the orientation of the polar headgroup to a perpendicular arrangement with respect to the air/solution interface. The smaller bands located at 1173 and 1170 cm^{-1} in the absence and presence of RBT, respectively, are ascribed to the asymmetric stretching mode of the C−O−C group of the DPPC phospholipid, i.e., carbon atoms above the polar headgroup, as the bands appear in both cases. Therefore, the contribution of the C−O−C group of the RBT molecule to the PM-IRRAS signal can be considered not significant.[29] This band is also reversed upon interaction of the DPPC with the RBT, indicating a large conformational change of the polar headgroup.

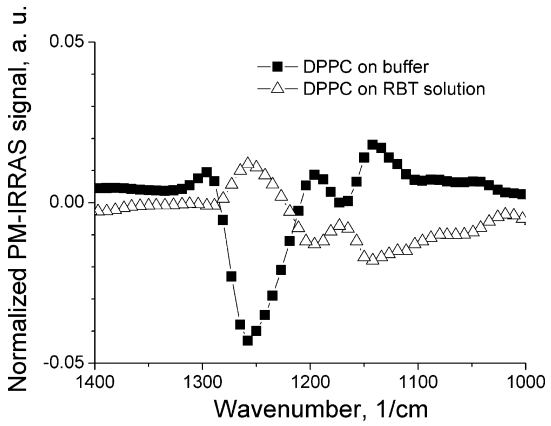

Figure 12. PM-IRRAS spectra of the phosphate and the C−O−C group vibrations region of a DPPC monolayer on a phosphate buffer subphase (black squares) and on a phosphate buffer containing 0.12 μM of RBT subphase (empty triangles) recorded at a surface pressure of 30 mN/m.

CONCLUSIONS

Although some data can be found in the literature about the interaction of RBT with lipid membranes, less attention has been paid to the possible effect of this drug on a physiological protective barrier: the lung surfactant. To our knowledge, this is the first report toward the study of RBT with monolayers of the zwitterionic DPPC and the anionic DPPG phospholipids used as mimetic models for the phospholipid content of lung surfactants. The presence of the RBT molecule at the phospholipid Langmuir monolayer was revealed by a significant expansion in the $\pi-A$ isotherms. Results also pointed to a total recovery of the amount of RBT at the phospholipid monolayer after two subsequent compressions cycles of the monolayer. Finally, computer simulations suggest that the interactions between RBT and the DPPC and DPPG Langmuir monolayers can be described as the formation of an inclusion complex. This formed complex has an important implication preventing the penetration of the RBT into the alkyl chain region of the phospholipids, leading to a disruption of the monolayer structure and a possible toxicological effect.

AUTHOR INFORMATION

Corresponding Author

*E-mail: mlucio@ff.up.pt, jjginer@uco.es. Fax/Tel: +34 957 218 618.

Notes

The authors declare no competing financial interest.

ACKNOWLEDGMENTS

The authors thank the Spanish CICYT for financial support of this research in the framework of Projects CTQ2010-17481 and also thank the Junta de Andalucía (Consejería de Innovacion, Ciencia y Empresa) for special financial support (P08-FQM-4011 and P10-FQM-6703). Authors are also grateful to the FCT for financial support under Project PTDC/QUI-QUI/101022/2008 with coparticipation European Community funds from the FEDER, QREN, and COMPET. We thank Carlos Rubia-Paya for invaluable help with the experiments. J.J.G.-C. acknowledges Alexander von Humboldt foundation for a postdoctoral fellowship. M.P. and J.M.C. thank

FCT (Lisbon) for the fellowships (SFRH/BD/63318/2009 and SFRH/BD/66789/2009, respectively).

REFERENCES

(1) Global tuberculosis control: WHO report 2011; World Health Organization: France, 2011.
(2) Corbett, E. L.; Watt, C. J.; Walker, N.; Maher, D.; Williams, B. G.; Raviglione, M. C.; Dye, C. *Arch. Intern. Med.* **2003**, *163*, 1009−1021.
(3) DeJong, C. B.; Israelski, D. M.; Corbett, E. L.; Small, P. M. *Ann. Rev. Med.* **2004**, *55*, 283−301.
(4) Figueiredo, R.; Moiteiro, C.; Medeiros, M. A.; Almeida da Silva, P.; Ramos, D.; Spies, F.; Ribeiro, M. O.; Lourenço, M. C. S.; Júnior, I. N.; Gaspar, M. M.; et al. *Bioorg. Med. Chem.* **2009**, *17*, 503−511.
(5) King, R. J.; Clements, J. A. *Am. J. Physiol.* **1972**, *223*, 715−726.
(6) Harwood, J. L. *Prog. Lipid Res.* **1987**, *26*, 211−256.
(7) Cochrane, C. G.; Revak, S. D. *Science* **1991**, *254*, 566−568.
(8) Schurch, S.; Goerke, J.; Clements, J. A. *Proc. Natl. Acad. Sci. U.S.A.* **1976**, *73*, 4698−4702.
(9) Vostrikov, V. V.; Selishcheva, A. A.; Sorokoumova, G. M.; Shakina, Y. N.; Shvets, V. I.; Savel'ev, O. Y.; Polshakov, V. I. *Eur. J. Pharm. Biopharm.* **2008**, *68*, 400−405.
(10) Shakina, Y. N.; Vostrikov, V. V.; Sorokoumova, G. M.; Selishcheva, A. A.; Shvets, V. I. *Bull. Exp. Biol. Med.* **2005**, *140*, 711−713.
(11) Shelly, S., A.; Balis, J. U.; Paciga, J. E.; Espinoza, C. G.; Richman, A. V. *Lung* **1982**, *160*, 195−206.
(12) HyperChem 7.51; Hypercube, Inc.: Gainesville, FL.
(13) Van der Heyden, A.; Regnouf-de-Vains, J.-B.; Warszynski, P.; Dalbavie, J.-O.; Zywocinski, A.; Rogalska, E. *Langmuir* **2002**, *18*, 8854−8861.
(14) Kane, P.; Fayne, D.; Diamond, D.; Bell, S. E. J.; McKervey, M. A. *J. Mol. Model.* **1998**, *4*, 259−267.
(15) Hönig, D.; Möbius, D. *J. Phys. Chem.* **1991**, *95*, 4590−4592.
(16) Fainerman, V. B.; Zhao, J.; Vollhardt, D.; Makievski, A. V.; Li, J. B. *J. Phys. Chem. B* **1999**, *103*, 8998−9007.
(17) Deng, J.; Hottle, J. R.; Polidan, J. T.; Kim, H.-J.; Farmer-Creely, C. E.; Viers, B. D.; Esker, A. R. *Langmuir* **2004**, *20*, 109−115.
(18) Deng, J.; Polidan, J. T.; Hottle, J. R.; Farmer-Creely, C. E.; Viers, B. D.; Esker, A. R. *J. Am. Chem. Soc.* **2002**, *124*, 15194−15195.
(19) Deng, J.; Viers, B. D.; Esker, A. R.; Anseth, J. W.; Fuller, G. G. *Langmuir* **2005**, *21*, 2375−2385.
(20) Thirumoorthy, K.; Nandi, N.; Vollhardt, D. *Langmuir* **2007**, *23*, 6991−6996.
(21) Chen, X.; Huang, Z.; Hua, W.; Castada, H.; Allen, H. C. *Langmuir* **2010**, *26*, 18902−18908.
(22) Roldán-Carmona, C.; Giner-Casares, J. J.; Pérez-Morales, M.; Martín-Romero, M. T.; Camacho, L. *Adv. Colloid Interface Sci.* **2012**, *173*, 12−22.
(23) Grüniger, H.; Möbius, D.; Meyer, H. *J. Chem. Phys.* **1983**, *79*, 3701−3710.
(24) Giner-Casares, J. J.; Pérez-Morales, M.; Bolink, H. J.; Muñoz, E.; de Miguel, G.; Martín-Romero, M. T.; Camacho, L. *J. Colloid Interface Sci.* **2007**, *315*, 278−286.
(25) Casey, M. L.; Whitlock, H. W. *J. Am. Chem. Soc.* **1975**, *97*, 6231−6236.
(26) Mendelsohn, R.; Brauner, J. W.; Gericke, A. *Annu. Rev. Phys. Chem.* **1995**, *46*, 305−334.
(27) Aroti, A.; Leontidis, E.; Maltseva, E.; Brezesinski, G. *J. Phys. Chem. B* **2004**, *108*, 15238−15245.
(28) Blaudez, D.; Turlet, J. M.; Dufourcq, J.; Bard, D.; Buffeteau, T.; Desbat, B. *J . Chem. Soc., Faraday Trans.* **1996**, *92*, 525−530.
(29) Zawisza, I.; Wittstock, G.; Boukherroub, R.; Szunerits, S. *Langmuir* **2008**, *24*, 3922−3929.
(30) Blaudez, D.; Buffeteau, T.; Cornut, J. C.; Desbat, B.; Escafre, N.; Pezolet, M.; Turlet, J. M. *Appl. Spectrosc.* **1993**, *47*, 869−874.